The Visual Computer (2021) 37:2173–2194
https://doi.org/10.1007/s00371-020-01978-3

ORIGINAL ARTICLE

Enhanced holoentropy-based encoding via whale optimization for highly efficient video coding

Venkatesh Munagala[1] · **Satya Prasad Kodati**[1]

Accepted: 8 September 2020 / Published online: 8 October 2020

Abstract
High-efficiency video coding (HEVC), a video compression method is considered as the most capable descendant of the extensively deployed advanced VC (AVC). Compared with AVC, HEVC provides about twice the data compression ratio at the similar video quality level or considerably enhanced video quality at an equal bit rate. This paper proposes a novel enhanced holoentropy model for proficient systems for distributed VC (DVC). HEVC standard is considered as an archetypal system. The main contribution of this paper is the accomplishment of the encoding process in the HEVC system by enhanced holoentropy, which is linked with the proposed weighting tansig function. It necessitates considerable development when handling video sequences with high resolution. The pixel deviations under altering frames are grouped based on interest, and the outliers are eliminated with the aid of an enhanced entropy standard known as enhanced holoentropy. Here, the weight of tansig function is optimally tuned by whale optimization algorithm. To next of implementation, the suggested encoding scheme is compared with the conventional schemes concerning the number of compressed bits and computational time. By carrying out the encoding process, it reduces the video size with perceptually improved video quality or PSNR.

Keywords HEVC · Holoentropy · Weighting tansig function · PSNR · Whale optimization

Abbreviations

ABC	Artificial bee colony
AMVP	Advanced MV prediction
AVC	Advanced VC
BE	Blind extraction
CABAC	Context-adaptive binary arithmetic coding
CB	Coding blocks
CM	Context modeling
CTB	Chroma tree block
CTU	Coding tree unit
CU	Coding unit
CPMV	Control point motion vectors
DSCNN	Decoder-side scalable convolutional neural network
DVC	Distributed VC
FF	Fire fly
GA	Genetic algorithm
HEVC	High efficiency video coding
IPL	Inter-picture prediction loop
IRAP	Intra-random access point
JCT-VC	Joint collaborative team on video coding
JND	Just noticeable distortion
LC	Luma coding
LDP	Low delay power
MB	Macro block
MVD	Multi-view video plus depth
MPEG	Moving picture experts group
MPRGAN	Multi-level progressive refinement network via an adversarial training approach
MCMC	Markov Chain Monte Carlo
MC	Motion compensation
MV	Motion vector
NN	Neural network
NTC	Nonzero transform coefficient
PAMC	Perspective affine motion compensation
PB	Prediction blocks
PSNR	Peak signal-to-noise ratio
PSO	Particle swarm optimization
QP	Quantization parameter

✉ Venkatesh Munagala
venkatesh4research@gmail.com

Satya Prasad Kodati
prasad_kodati@yahoo.co.in

[1] JNTUK, Kakinada, Andhra Pradesh, India

RMSE	Root mean squared error
UQI	Universal quality image index
VIF	Visual information fidelity
PU	Prediction units
RD	Rate distortion
RA	Random access
SAO	Sample adaptive offset
SSIM	Structural similarity index
SVR	Support vector regression
TB	Transform blocks
TU	Transform units
VBR	Video bit rate
VCS	Video constraint set
VVC	Versatile video coding
VCEG	Video coding experts group
WOA	Whale optimization algorithm
3D-HEVC	Three-dimensional HEVC

1 Introduction

HEVC is the novel VC standard developed in most recent times, and the improvement of this novel scheme was enthused by the requirement of video sequences with high resolution ahead of HD and for developments at the framework level [1–5]. It comprises of numerous coding equipments like CU, PU, and CTB partitioning device [6–8]. The process of HEVC is initiated by partitioning the image into a variety of blocks by quad tree mechanism followed by prediction and coding [9–11]. The intra-coding scheme in HEVC offers quality coding of videos. Accordingly, the HEVC performs better than the traditional VC standards [12, 13].

HEVC offers enhanced compression ratio and assistance for discriminated and multi-view encoding and premium 4 K content for online and broadcast retailers to offer additional content channels on conventional delivery channels [14–16]. For reducing the visual impacts and performance overheads, a solution for watermarking and encryption compliant with HEVC criterions is premeditated [17]. The evaluation of video quality could be categorized into objective and subjective quality measurements. The subjective evaluation is real and influential. Nevertheless, subjective quality estimation necessitates an enormous attempt to create an environment to estimate the quality of a video.

HEVC is currently being prepared as the newest video coding standard of the ITU-T Video Coding Experts Group and the ISO/IEC Moving Picture Experts Group [18–20]. The main goal of the HEVC standardization effort is to enable significantly improved compression performance relative to existing standards—in the range of 50% bit rate reduction for equal perceptual video quality [10]. The HEVC standard is the most recent joint video project of the ITU-T VCEG and the ISO/IEC MPEG standardization organizations, working together in a partnership known as the JCT [21–23]. There is no single coding element in the HEVC design that provides the majority of its significant improvement in compression efficiency in relation to prior video coding standards [24–26].

The main contribution of the presented model is listed below:

- Introduces encoding process in HEVC system by enhanced holoentropy, which is linked with the proposed weighting tansig function.
- The pixel deviations under altering frames are grouped on the basis of interest, and the outliers are eliminated with the aid of an enhanced entropy standard known as enhanced holoentropy.
- The weight of tansig function is optimally tuned by whale optimization algorithm (WOA) for optimization purpose.

The paper is organized as follows. Section 2 portrays the related works reviewed under this topic. Section 3 demonstrates the modeling of HEVC: standard architecture with description and Sect. 4 portrays the enhanced holoentropy-based encoding for HEVC by WOA. Moreover, Sect. 5 explains the results and Sect. 6 concludes the paper.

2 Literature survey

2.1 Related works

Kalyan et al. [27] have established an approach depending on the detection of homogeneous and motionless texture-dependent areas in a specified format. Entropy is measured as an element for the examination of CU texture. An entropy differentiation among CU's was designed for recognition of stationary areas in a video format.

Tanima and Hari [28] suggested a robust structure with a BE procedure for HEVC standards. A "readable watermark" was implanted imperceptibly in expected blocks of the video sequence. The experimental outcomes reveal that the anticipated work limits the augment in VBR and deprivation of perceptual quality.

Zhang et al. [29] implemented a fast 3D-HEVC encoder approach dependent on the depth map correlation and texture video to lessen computational complications. As the depth map and video texture correspond to a similar prospect at a similar time interval, it was not proficient to exploit the entire prediction modes in the adopted scheme.

Lin et al. [30] suggested a compressed video representation to forecast the SSIM metrics for HEVC and AVC videos. The representation adopted was SVR design. Moreover, the encoding decisions were only deployed while estimate the motions to carry out the prediction, and it does not require the data from the pixel domain

Guo et al. [31] established a method that measures not only the video content but also measures the position and significance of the corrupted portion and implements a hierarchical significance-dependent video quality evaluation. Accordingly, simulations were held to enumerate the hierarchical significance of corrupted content.

Shanshe Wang et al. [32] introduced an enhanced technique that intends to minimize the performance complication of 3D-HEVC. The fundamental inspiration of the suggested mechanism was to exploit the depth map variation feature.

Xiem et al. [33] suggested a new scalable VC solution by hybridizing the DVC techniques using a distributed coding layer and HEVC-compliant base layers. The suggested model tempts to offer reduced encoding intricacy and error while attaining an increased rate of compression.

Sunil Kumar et al. [34] suggested a scheme to enhance the benchmark entropy by establishing the optimized weighting constraints. According to the adopted scheme, an improved compression rate could be obtained over the benchmark entropy encoding. In addition, the optimization was carried out using the FF algorithm in recent times. Moreover, the trials were done for PSNR evaluation for altering the rate of data transmission.

In 2019, Choi et al. [35] have proposed an efficient perspective affine motion estimation/compensation for VVC standard. The PAMC method which can cope with more complex motions such as shear and shape distortion utilized perspective and affine motion model. The PAMC method uses four CPMVs to give degree of freedom to all four corner vertices. Besides, the proposed algorithm is integrated into the AMC structure so that the existing affine mode and the proposed perspective mode can be executed adaptively. The experimental results show that the BD rate reduction of the proposed technique can be achieved up to 0.45% and 0.30% on Y component for RA and LDP configurations, respectively.

In 2019, Yang et al. [36] have introduced a DSCNN approach to achieve quality enhancement for HEVC, which does not require any modification of the encoder. In particular, our DSCNN approach learns a model of CNN to reduce distortion of both I and B/P frames in HEVC. Furthermore, a scalable structure is included in our DSCNN, such that the computational complexity of our DSCNN approach is adjustable to the changing computational resources. Finally, the experimental results show the effectiveness of our DSCNN approach in enhancing quality for both I and B/P frames of HEVC.

In 2020, Lee et al. [37] have determined an efficient color artifact removal algorithm based on HEVC for high-dynamic range video sequences. A block-level QP offset-control-based efficient compression algorithm for the HDR sequence was proposed. The candidate CUs with the annoying area to the human eye based on the JND model were extracted. Subsequently, the chromatic distorted blocks are verified by the activity function as the chromatic artifact is observed at the nearby strong edge. Therefore, the proposed method provides pleasant viewing results by eliminating annoying color distortions and has better frame clarity, and compression efficiency in terms of video coding.

In 2018, Kalyan et al. [38] have established a fast HEVC scheme based on Markov Chain Monte Carlo model and Bayesian classifier. A novel way considering skip detection and CU termination as two-class decision-making problems in which Bayesian classifier is used for both of these approaches. Prior and class conditional probability values for a Bayesian classifier are not known at the time of encoding a video frame. Experimental results show that the proposed method provides significant time reduction for encoding with reasonably low loss in video quality.

In 2018, Jin et al. [39] have determined a novel post-processing technique using MPRGAN, for artifacts reduction and coding efficiency improvement in intra-frame coding. Furthermore, our network generates multi-level residues in one feed-forward pass through the progressive reconstruction. This coarse-to-fine work fashion, which makes our network have high flexibility, can make trade-off between enhanced quality and computational complexity. Extensive evaluations on benchmark datasets verify the superiority of our proposed MPRGAN model over the latest state-of-the-art methods with fast deployment running speed.

In 2018, Young et al. [40] have suggested a scheme to improve the visual quality of the video coding standard. We apply a CNN model to HEVC encoding system and suggest a combined coding scheme using a CNN model. The deterioration of the quality caused by compression can be improved through CNN, which does not require much computational complexity. Through experiment, we verify that the proposed scheme achieves up to 0.24 dB of the quality improvement on HM 16.10 reference software.

2.2 Review

Table 1 shows the methods, features, and challenges of conventional techniques based on HEVC encoding. At first, AMP was implemented in [27] that necessitates a lower bit rate along with minimized time for encoding. However, possibilities of error could be found that remains as a drawback for this scheme. In addition, video watermarking was deployed in [28], which offers better effectiveness with minimized computational complexity. However, there was no implementation on compressed domain watermarking using different codes. Moreover, the Mode decision scheme was suggested in [29] that offers reduced complexity with fast texture VC, but there were chances for false edge occurrence that reduces the accuracy. Also, SVR was implemented in [30], which minimizes the complexity, and there was

Table 1 Review of conventional HEVC techniques

References	Adopted methodology	Features	Challenges
Goswami et al. [27]	AMP	Necessitates a lower bit rate Minimized time for encoding	Possibilities of error
Dutta and Gupta [28]	Video watermarking	Offers better effectiveness Reduces the computational complexity	No implementation on compressed domain watermarking using different codec's
Zhang et al. [29]	Mode decision scheme	Reduces the computational complexity Offers fast texture VC	Chances for false edge occurrence that reduces the accuracy
Lin et al. [30]	SVR	Reduced computation complexity No need for decoding the entire bitstream	No exploration of various characteristics of HEVC and AVC
Guo et al. [31]	NN	Increased accuracy Better prediction of video quality	It does not involve temporal features
Wang et al. [32]	Mode decision scheme	Reduced complexity Minimized rate distortion loss	Complex depth region
Van et al. [33]	DVC	Reduced complexity Increased scalability Increased RD performance	Requires implementation on the correlation process
Sunil Kumar et al. [34]	FF	Minimized performance complications Better reliability	Compression effectiveness has to be enhanced more.
Choi et al. [35]	PAMC Method	Low delay BD rate reduction Improved effectiveness	The higher-order motion models should be investigated and applied for three-dimensional modeling of motion
Yang et al. [36]	DSCNN approach	Better performance Low computational complexity Quality enhancement	Need to achieve computation-scalable quality enhancement for decoded images or videos that adapt to the varying computational resources
Lee et al. [37]	HDR technique	Average gain Increased bit rate Better frame clarity compression efficiency	The existence of a strong luminance edge does not necessarily coincide with a strong chrominance edge
Kalyan et al. [38]	Markov Chain Monte Carlo (MCMC) model	Significant time reduction for encoding Low loss in video quality More robust and adaptive in nature	HEVC is a high degree of computational complex
Jin et al. [39]	MPRGAN	High flexibility Superior performance Adjustable to resource-aware applications	To simplify the network while boosting its visual quality and extend the methodology to more related applications
Young et al. [40]	CNN model	Low computational complexity Higher PSNR	Improving the overall compression performance by improving the quality of inter-frame coding

no necessitation for decoding the entire bitstream. However, there was no exploration of various characteristics of HEVC and AVC. In [31], NN was exploited that increases the accuracy with better prediction of video quality. However, it does not involve the temporal features. Moreover, the Mode decision scheme was employed in [32], which provides minimized complexity and rate distortion loss, but the computation of depth region is complex. In addition, DVC was suggested in [33], which offers minimized complications with increased scalability and RD performance. However, it requires the implementation of the correlation process. Finally, FF was exploited in [34] that offer minimized performance complications with increased reliability. However, the compression effectiveness has to be enhanced more. PAMC method was implemented in [35] that have low delay, BD rate reduction and improved effectiveness. However, the higher-order motion models should be investigated and applied for three-dimensional modeling of motion. In addition, DSCNN approach was deployed in [36], which offers better performance, low computational complexity and quality enhancement. However, there is need to achieve computation-scalable quality enhancement for decoded images or videos that adapt to the varying computational resources. Moreover, HDR technique was suggested in [37] that offer average gain, increased bit rate, better frame clarity and compression efficiency, but the existence of a strong luminance edge does not necessarily coincide with a strong chrominance edge. Also, MCMC model was implemented in [38] involving significant time reduction for encoding, low loss in video quality, more robust and adaptive in nature. However, HEVC has high degree of computational complex. In [39], MPRGAN was exploited that high flexibility, superior performance and adjustable to resource-aware applications. However, there is need to simplify the network

while boosting its visual quality and extend the methodology to more related applications. Moreover, CNN model was employed in [40], which provides low computational complexity and higher PSNR, but needs to improve the overall compression performance by improving the quality of inter-frame coding. Thus the challenges in various techniques have to be solved to improve the HEVC performance.

3 Modeling of HEVC: standard architecture with description

3.1 CABAC standard

HEVC utilizes a single entropy coding technique that is customized by counting the characteristics, namely coefficient coding, adaptive coefficient scanning, and CM, which is identified as CABAC. For raising the effectiveness of CABAC coding, CM is carried out. The CM indicators are obtained using the partitioning depth of transform tree or coding. The syntax components of the indices consist of unit-flag; skip flag, spli-coding, cbf-cr, cbf-luma, split-transform-flag and cbf-cb. The information is reduced for increasing throughput using HEVC along with the bypass approach of CABAC. Horizontal, vertical and decent scans are types of scanning techniques, which are done in 4×4 sub-blocks in the entire size of TB.

The HEVC include the capability to convey the location of the final NTC, sign bits, a noteworthy map, and stages of the TC. The significance map is deployed for sub-blocks of 4×4, and a group flag pointing out an NTC group is conveyed to the entire clusters that contain a coefficient before the final coefficient position. The sign bit of the initial NTC is assumed from the uniformity of whole amplitudes while the "sign data hiding" along with two NTC in a 4×4 block and distinction between the scan directions of initial and final NTC is higher than three.

Figure 1 demonstrates the architecture diagram of HEVC. The HEVC [15, 16] scheme deploys inter- and intra-picture prediction models, which is dependent on the theory of the "video compression" principles. In the initial sequence of the video, the intra-picture prediction method is deployed to find out the spatial significance among the frame sections. The inter-picture prediction model portrays an MV and a reference frame depending on the association among the frames. The proposed MV is utilized to envisage the block samples of all the frames by mode decision data and MC. The coefficients of conversion obtained as a result are offered to entropy encoding, scaling, and quantization. The encoder includes a replicated decoder phase via which the reverse procedures of transformation and scaling are carried out to restructure the estimated left over the signal. The buffer accumulates the replica of the output of the decoder, and it is exploited to forecast the following frames. The combined VC context comprises numerous appealing characteristics, and constructive mechanisms like CU and CB, CTU and CTB, TU and TB, PU and PB, MC, MV signaling and so on.

The CTU is equal to the MB of the preceding coding principles. On the other hand, the CTU size is usually superior to the MB. In addition, the CTB includes luma and syntax elements and the related chroma CTBs. In general, the luma CTBs are huge in dimension and therefore it is divided into small blocks using quadtrees-like signaling and tree structure. The positions and size of chroma and luma CTBs of a CTU are generally described by the quad tree syntax. A CTB might contain either segregated multi-CUs or single CU. Every CU can be divided into TUs and PUs. The TU and PU encompass its origin at the level of CU. The PBsis utilized to envisage CB's after the dividing process. The residual of luma CB is usually equal to luma TB, or it could be isolated into slighter luma TB's.

The MV in HEVC integrates AMVP which is obtained from both PBs concerning spatial and temporal functions. However, partial sample locations with six-tap filtering are deployed for MV in "H.264/MPEG-4AVC". In addition, numerous images are exploited in HEVC. HEVC considers thirty-three directional modes while evaluating intra-picture, in which 8 are acknowledged in "H.264/MPEG-4AVC." The prediction directions prefer the intra-picture prediction encoding based on formerly decoded adjacent PBs.

Several alterations are performed in the CABAC escalating the compression performance in HEVC for better throughput and to reduce the context recall needs, and it is deployed for entropy coding. Similar to "H.264/MPEG-4AVC," the deblocking filter functioned in the IPL remnants similar for HEVC. The operational outline is obstructed for filtering and decision-making procedure. Further than the deblocking filter, a "nonlinear amplitude mapping" is exploited in IPL. The major intention lies in reconstructing the amplitudes of signal with a look-up table that is described with novel constraints, which could be approximated using the histogram scrutiny close to the encoder side.

3.2 Enhancement model

CABAC is considered a throughput bottle neck in the VC model. On considering the count of bins that it practices for each second, the CABAC throughput could be evaluated. A rise in the number of bins will be almost equivalent to the rise in throughput. However, it is much complicated to deal with numerous bins analogous in CABAC. On concerning recursive time partition, the modified range is provided, and for accurate possibility approximation, the modified framework is provided. The assortment of context is made based on the kind of syntax and binIdx constituent. The range update and feedback loops-context updates were much effortlessly

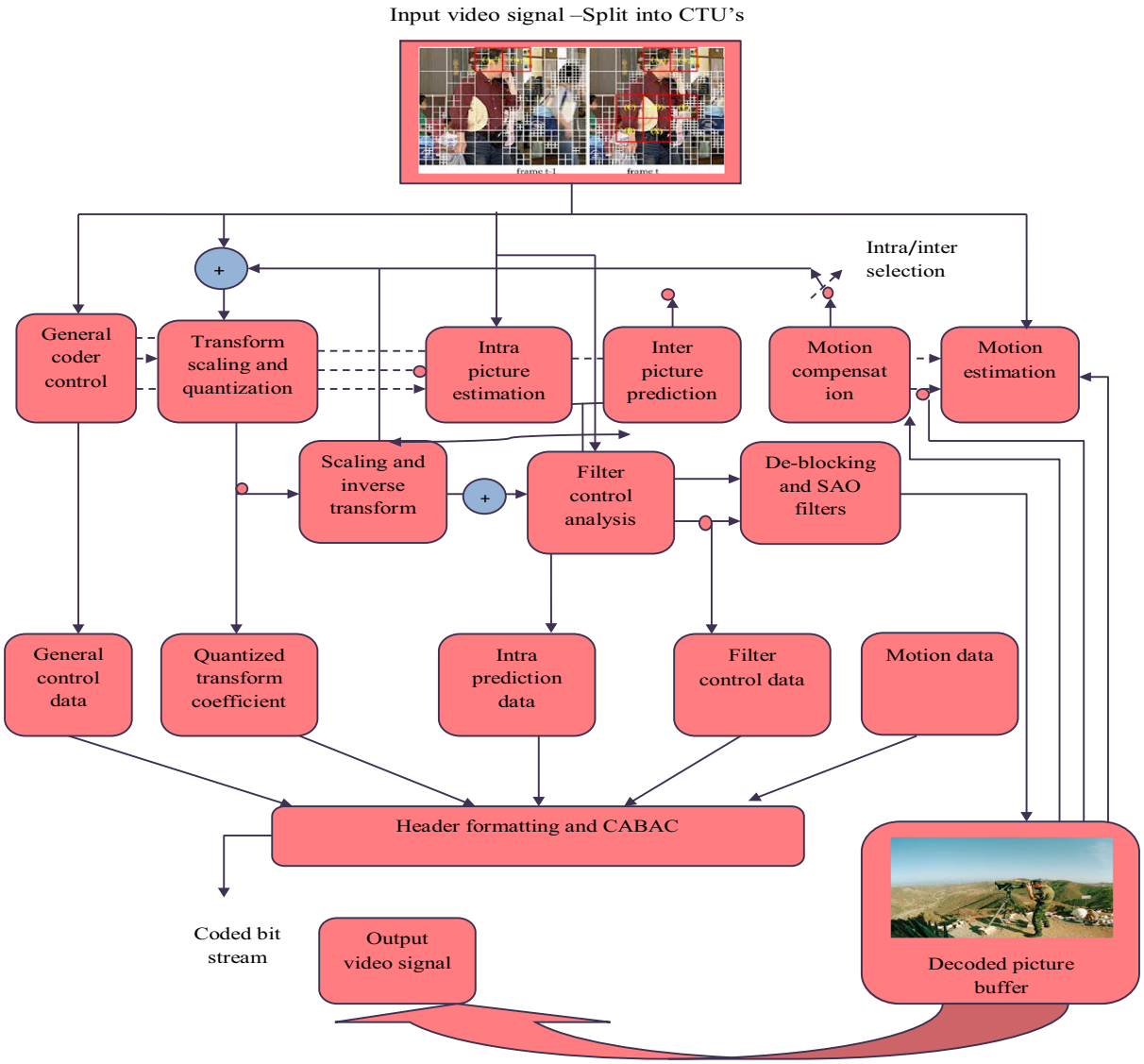

Fig. 1 Pictorial representation of HEVC encoder

comprehended when compared with the context assortment loops. The calculation attempts are required if bin context is based on the various erstwhile bin values. Consequently, it's an identified actuality that throughput blockage is owing to the bin based on context assortment.

The throughput crisis of CABAC has to be solved, which is a significant task. A variety of techniques are made for enhancing the throughput along with the least loss of coding. With the minimization of context coded bins, it was simpler to practice the coded bins in analogous, and as a result, the throughput could be enhanced. By means of "group bypass coded bins" practiced in similar rounds, the bins were rearranged to increase the probability of numerous bins developed in HEVC. Therefore, for this action, the tentative computation is essential. If bins are incorporated with altering context and its assortment logic, the quantity of tentative totaling increases and therefore to minimize it, the bins have to be rearranged. Hence, the throughput is augmented mechanically with reduced power convention. By minimizing the context assortment reliance, the entire amount of bins, parsing memory and reliance needs, throughput could be minimized with reduced cost and power. The entire amount of bins is minimized by deducing the values of the bin, evading signaling out moded bins and varying binarization by deploying advanced level flags. "Parsing" is the reason for minimized throughput, and hence, it has to be decoupled from various executions. Reducing memory capability is essential for rising throughput.

Figure 2 demonstrates the proposed architecture by incorporating WOA and optimization process. The traditional block-dependent hybrid VC technique is deployed in HEVC before the standardization procedure. Numerous develop-

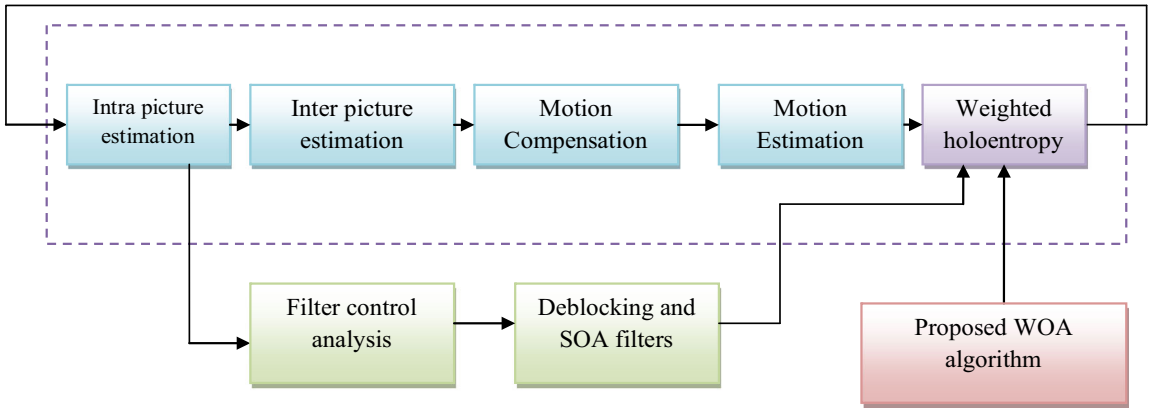

Fig. 2 Proposed architecture using WOA optimization algorithm

ments are done for structuring an HEVC method. In terms of color video signals, YCbCr color space will be deployed by HEVC that partition a color to three elements—(luma) Y indicates brightness and Cr and Cb symbolize the color variation from gray in the direction of red and blue correspondingly. The video images are split and sampled into CTU that comprises of luma CTBs and chroma CTBs. Moreover, CTU is exploited by HEVC for the decoding region. The CTBs are deployed as CBs and separated using quad tree syntax. The size of CB is reduced until the fitness is attained. By deploying residual quad tree, the CBs are separated into TB's. For enlarging the coding effectiveness, the HEVC deploys a TB to shift across a lot of PBs of inter-picture assumed CUs. The image is divided into numerous segments that are deployed deliberately for resynchronization following a data loss. In addition, HEVC strips are employed for facilitating the parallel processing framework for decoding and encoding. Moreover, the intra-picture and inter-picture predictions are carried out.

In intra-picture estimation, the decoded boundary samples of adjacent blocks are used as reference data for spatial prediction in regions where inter-picture prediction is not performed. Intra-picture prediction supports 33 directional modes (compared to eight such modes in H.264/MPEG-4 AVC), plus planar (surface fitting) and DC (flat) prediction modes. The selected intra-picture prediction modes are encoded by deriving most probable modes (e.g., prediction directions) based on those of previously decoded neighboring PBs. In inter-picture estimation, the PB partitioning is compared to intra-picture-predicted CBs; HEVC supports more PB partition shapes for inter-picture-predicted CBs. The samples of the PB for an intra-picture-predicted CB are obtained from those of a corresponding block region in the reference picture identified by a reference picture index, which is at a position displaced by the horizontal and vertical components of the motion vector. In motion compensation, the Quarter-sample precision is used for the MVs, and 7-tap or 8-tap filters are used for interpolation of fractional-sample positions (compared to six-tap filtering of half-sample positions followed by linear interpolation for quarter-sample positions in H.264/MPEG-4 AVC). As in H.264/MPEG-4 AVC, a scaling and offset operation may be applied to the prediction signal(s) in a manner known as weighted prediction. Furthermore, the encoder needs to perform motion estimation, which is one of the most computationally expensive operations in the encoder, and complexity is reduced by allowing a small number of candidates. When the reference index of the neighboring PU is not equal to that of the current PU, a scaled version of the motion vector is used. In HEVC, the processing order of the deblocking filter is defined as horizontal filtering for vertical edges for the entire picture was followed by vertical filtering for horizontal edges. This specific order enables either multiple horizontal filtering or vertical filtering processes to be applied in parallel threads or can still be implemented on a CTB-by-CTB basis with only a small processing latency. The deblocking filter is applied to all samples adjacent to a PU or TU boundary except the case when the boundary is also a picture boundary or when deblocking is disabled across slice or tile boundaries. It should be noted that both PU and TU boundaries should be considered since PU boundaries are not always aligned with TU boundaries in some cases of inter-picture-predicted CBs. SAO is a process that modifies the decoded samples by conditionally adding an offset value to each sample after the application of the deblocking filter, based on values in look-up tables transmitted by the encoder. SAO filtering is performed on a region basis, based on a filtering type selected per CTB by a syntax element. As in H.264/MPEG-4 AVC, a scaling and offset operation may be applied to the prediction signal(s) in a manner known as weighted prediction. At this point in the process, that weighted prediction is applied when selected by the encoder. Whereas H.264/MPEG-4 AVC supported both temporally implicit and explicit weighted prediction, in HEVC only explicit weighted prediction is applied, by scal-

ing and offsetting the prediction with values sent explicitly by the encoder.

3.3 Probability estimation

Context modeling: The bin value in CABAC is processed depending on the related coding mode decisions, namely regular or bypass mode. The later one is predominantly preferred than the former one for CM.

Probability assignment and estimation: The probabilistic scheme of CABAC is based on the adaptive constraints of bin source that performs on a "bin-by-bin basis" in the harmonized and adaptive manner (backward) in decoding and encoding procedure. The whole procedure is denoted as probability estimation, which is given by Eq. (1),

$$p_{\mathrm{SL}}^{(t+1)} = \begin{cases} a * p_{\mathrm{SL}}^{(t)}, & \text{if } b = \upsilon_{\mathrm{SM}}, \text{ i.e., an SM occurs} \\ 1 - a * \left(1 - p_{\mathrm{SL}}^{t}\right), & \text{otherwise} \end{cases} \tag{1}$$

where t time interval, a indicates scaling factor, b indicates bin, p_{SL} indicates of least probable sign, and p_{ML} indicates the probability of most probable sign.

4 Enhanced Holoentropy-based encoding for HEVC by whale optimization algorithm

4.1 Proposed holoentropy for CABAC

Entropy measurement for detecting outliers is not sufficient. The total correlation is also necessary to get better outlier candidates. Likewise, contribution of holoentropy along with entropy and total correlation helps in giving appropriate results for outlier detection. The holoentropy is defined as the sum of entropy and total correlation of random vector Y. Here, $HLx(Y)$ can be expressed using Eq. (2).

$$HLx(Y) = Hx(Y) + Cx(Y) \tag{2}$$

where $Cx(Y)$ indicates the total correlation and $Hx(Y)$ indicates the total entropy. However, this paper proposes a nonlinear relationship operator to determine the correlation, rather than statistical correlation function. Moreover, the nonlinear relationship operator is further intended to tune by advanced soft computing algorithm called as WOA.

The formulation of holoentropy is given by Eq. (3), where the weighted tansig function, $w_x(i)$ is determined using Eq. (4) in which $i = 1, \ldots N$.

$$HL = \sum w_x(i) \times E_i \tag{3}$$

$$w_x(i) = 2\left(1 - \frac{1}{1 + \exp(-E_i)}\right) \tag{4}$$

where E_i denotes the ith entropy value.

The term peak signal-to-noise ratio (PSNR) is an expression for the ratio between the maximum possible value (power) of a signal and the power of distorting noise that affects the quality of its representation. For color images with three RGB values per pixel, the definition of PSNR is the same except the MSE is the sum over all squared value differences (now for each color, i.e., three times as many differences as in a monochrome image) divided by image size and by three. The PSNR block computes the peak signal-to-noise ratio, in decibels, between two images. This ratio is used as a quality measurement between the original and a compressed image. The higher the PSNR, the better the quality of the compressed or reconstructed image.

$$\mathrm{PSNR} = \frac{1}{N_v} \sum_{v=1}^{N_v} 10 \log_{10}\left(\frac{\mathrm{MAX}_I^2}{\mathrm{MSE}_v}\right) \tag{5}$$

In Eq. (5),$v = 1, 2, \ldots N_v$ in which N_v denotes the number of trial video sequences.MSE_v indicates the mean squared error value between the reconstructed trial video sequences and the original video sequence, andMAX_I is the maximum possible pixel value of the image and hence the pixels are represented using 8 bits per sample, (i.e., 255).

Here in the proposed framework, $w_x(i)$ is determined by factorizing the weighting function α_i with it as shown by Eq. (6).

$$w_x(i) = \alpha_i\, 2\left(1 - \frac{1}{1 + \exp(-E_i)}\right) \tag{6}$$

The weighting function, α_i has to be optimally tuned, for which the WOA optimization is exploited. Unlike other optimization algorithms, WOA uses a strong exploitation and exploration phase and its searching concept encircles the optimal point and so the convergence can be fast in less iterations. Hence it is considered to be well-suited for HEVC process, where high-resolution videos are encoded.

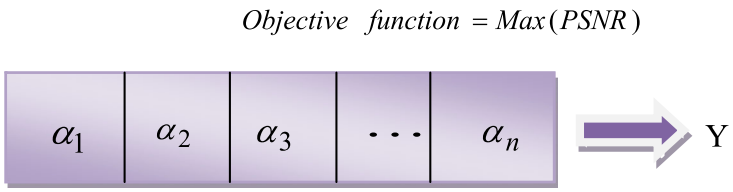

Fig. 3 Solution encoding

4.2 Objective model and solution encoding

The weight parameter, denoted by α_i, is given as input for solution encoding, in which i indicates the number of weights from 1 to n. The diagrammatic representation of solution encoding is shown in Fig. 3. Here, Y indicates the position vector in order to update the subsistence of an enhanced solution. Accordingly, the objective function of the proposed work is to maximize the PSNR as shown by Eq. (7).

$$\text{Objective function} = \text{Max(PSNR)} \tag{7}$$

4.3 Whale optimization algorithm

The weighting function α_i is given as input to the WOA model for fine-tuning. Whales are accountable for emotions, judgment, and social performances as made by humans [14]. The major motivating thing regarding the humpback whales is the marvelous hunting system. They could identify the location of prey and enclose them. Following the portrayal of the fine search agent, the erstwhile search agents will attempt to modernize their locations toward the optimal agent for search. This behavior is indicated by Eqs. (8) and (9), in which t points out the present iteration, coefficient vectors are signified by $\vec{A}$ and $\vec{C}$, and Y^* denotes the position vector of the most outstanding solution obtained so far; || indicates the absolute value,Y symbolizes the position vector, and '.' represents an element-by-element multiplication.

$$\vec{V} = \left|\vec{J}.\vec{Y}^*(t) - \vec{Y}(t)\right| \tag{8}$$

$$\vec{Y}(t+1) = \vec{Y}^*(t) - \vec{A}.\vec{V} \tag{9}$$

It is significant to note that Y^* has to be updated in the entire iterations in the subsistence of an enhanced solution. The vectors A and J are evaluated as in Eqs. (10) and (11) in which $\vec{f}$ is linearly reduced from two to zero for the course of iterations and $\vec{r}$ denotes a random vector in [0, 1].

$$\vec{A} = 2\vec{f}.\vec{r} - \vec{f} \tag{10}$$

$$\vec{J} = 2.\vec{r} \tag{11}$$

Exploitation phase: *Shrinking encircling mechanism*: This action is attained by reducing the value of $\vec{f}$ in Eq. (10). Observe that the distinction of $\vec{A}$ is further minimized by $\vec{f}$, that is $\vec{A}$ is an arbitrary value that lies among $\left[-\vec{f}, \vec{f}\right]$ in which $\vec{f}$ is minimized from two to zero for further iterations.

Spiral updating position: Initially, this technique valuates the distance found among the whale positioned at (Y, Z) and prey at (Y^*, Z^*). A spiral formula is also produced between the location of whale and prey as revealed in Eq. (12) in which $\vec{V}' = \left|\vec{Y}^*(t) - \vec{Y}(t)\right|$ and it denotes the distance of ith whale to prey, the variable for determining the shape of the logarithmic spiral is indicated by g, '.'refers to an element by element multiplication, and l is an alternate value that ranges between [− 1,1].

$$\vec{Y}(t+1) = \vec{V}.e^{gl}.\cos(2\pi l) + \vec{Y}^*(t) \tag{12}$$

It can be further designed as specified in Eq. (13) where p_a is an alternate number ranging between [0, 1], b is a constant for defining the shape of the logarithmic spiral.

$$\vec{Y}(t+1) = \begin{cases} \vec{Y}^*(t) - \vec{A} - \vec{V} & \text{if } p_a < 0.5 \\ \vec{V}'.e^{bl}.\cos(2\pi l) + \vec{Y}^*(t) & \text{if } p_a \geq 0.5 \end{cases} \tag{13}$$

Exploration phase: Here, an alternately chosen exploration agent rather than the best search agent is identified so far. This operation and $\left|\vec{A}\right| > 1$ highlights the exploration and permits the WOA method to carry out a wide-ranging

search. It is explained as in Eqs. (14) and (15), where $\vec{Y}_{rand}$ is a random whale selected from the present population.

Algorithm: Whale Optimization Algorithm

Assign the population of whales $Y_i(i = 1,2,....,n)$
Measure the fitness of all search agents
Y^* denotesthebest agent for search
While t is less than the number of iterations
  For every search agents
  Update $\vec{f}, A, J, l$ *and* p_a
    if 1 $p_a < 0.5$
      if 2 $(|A| < 1)$
        Update search agent position based on Eq. (9)
      else if 2 $(|A| \geq 1)$
        Choose an alternate search agent $\vec{Y}_{rand}$
        Update search agent position based on Eq. (15)
      end if 2
    else if 1 $p_a \geq 0.5$
      Update search agent position based on Eq. (13)
    end if 1
  end for
  Verify whether search agent extends above the search space
  Measure search agent fitness
  if there exists a better solution, update Y^*
  $t = t + 1$
end while
return Y^*

$$\vec{V} = \left| \vec{J}.\vec{Y}_{rand} - \vec{Y} \right| \tag{14}$$

$$\vec{Y}(t+1) = \vec{Y}_{rand} - \vec{A}.\vec{V} \tag{15}$$

5 Results and discussions

5.1 Simulation procedure

The proposed compression model using WOA for enhanced holoentropy depending on HEVC was implemented in JAVA, and the results were attained by exploiting 2 data sets. The data set 1 consist of the video in YUV file format such as Football, mobile, garden, coastguard, foreman, tennis, with a relevant count of sequences 125, 140, 115, 112, 300 and 300, which were obtained from (http://www.cipr.rpi.edu/resource/sequences/sif.html: Access date: 16-10-2018). The video sequences garden, Football, tennis, mobile, foreman and coast guards include a resolution of 352×240, and foreman and coastguard include a resolution of 352×288. The data set 2 is obtained from http://download.tsi.telecom-paristech.fr/gpac/dataset/dash/uhd/. Here, the video sequences such as UHD HEVC-720p-30 Hz, UHD HEVC-720p-60 Hz, UHD HEVC-1080p-30 Hz, UHD HEVC-1080p-60 Hz, UHD HEVC-2160p-30 Hz and UHD HEVC-2160p-60 Hz is used. This paper used the version 2 of HM software, which was established by the JCT-3 V to work on multi-view and 3D video coding extensions of HEVC and other video coding standards. It provides support for coding multiple views with inter-layer prediction. It is designed as a high-level syntax only extension to allow reuse of existing decoder components. The software can be accessible via https://hevc.hhi.fraunhofer.de/mvhevc. The performance of proposed and conventional compression models was validated by examining the PSNR of decoded video formats for

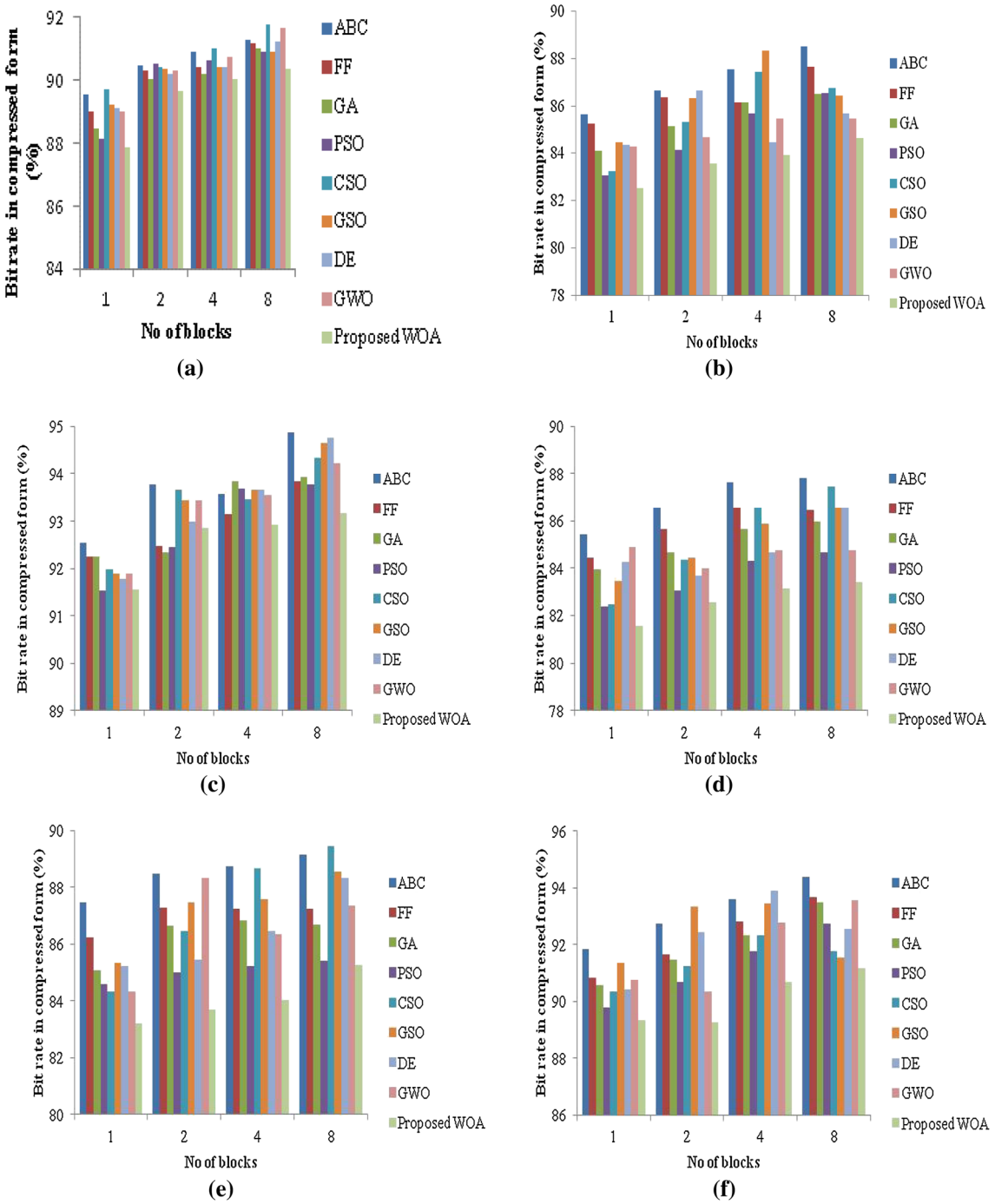

Fig. 4 Encoding performance of the proposed and conventional models with respect to bit rate in compressed form for data set 1. **a** Football, **b** mobile, **c** garden, **d** coastguard, **e** foreman and **f** tennis

a diverse count of encoded bits. The outcomes attained for the adopted scheme were distinguished with the traditional schemes like ABC [11], FF [41], GA [42], PSO [43], CSO [44], GSO [45], DE [46], and GWO [47].

5.2 Performance analysis

The performance of adopted enhanced holoentropy using WOA and other conventional algorithms with respect to PSNR value and the bit rate in compressed form for the entire collected video streams for data set 1 and 2 is specified in Figs. 4, 5, 6 and 7. Figure 4 shows the encoding

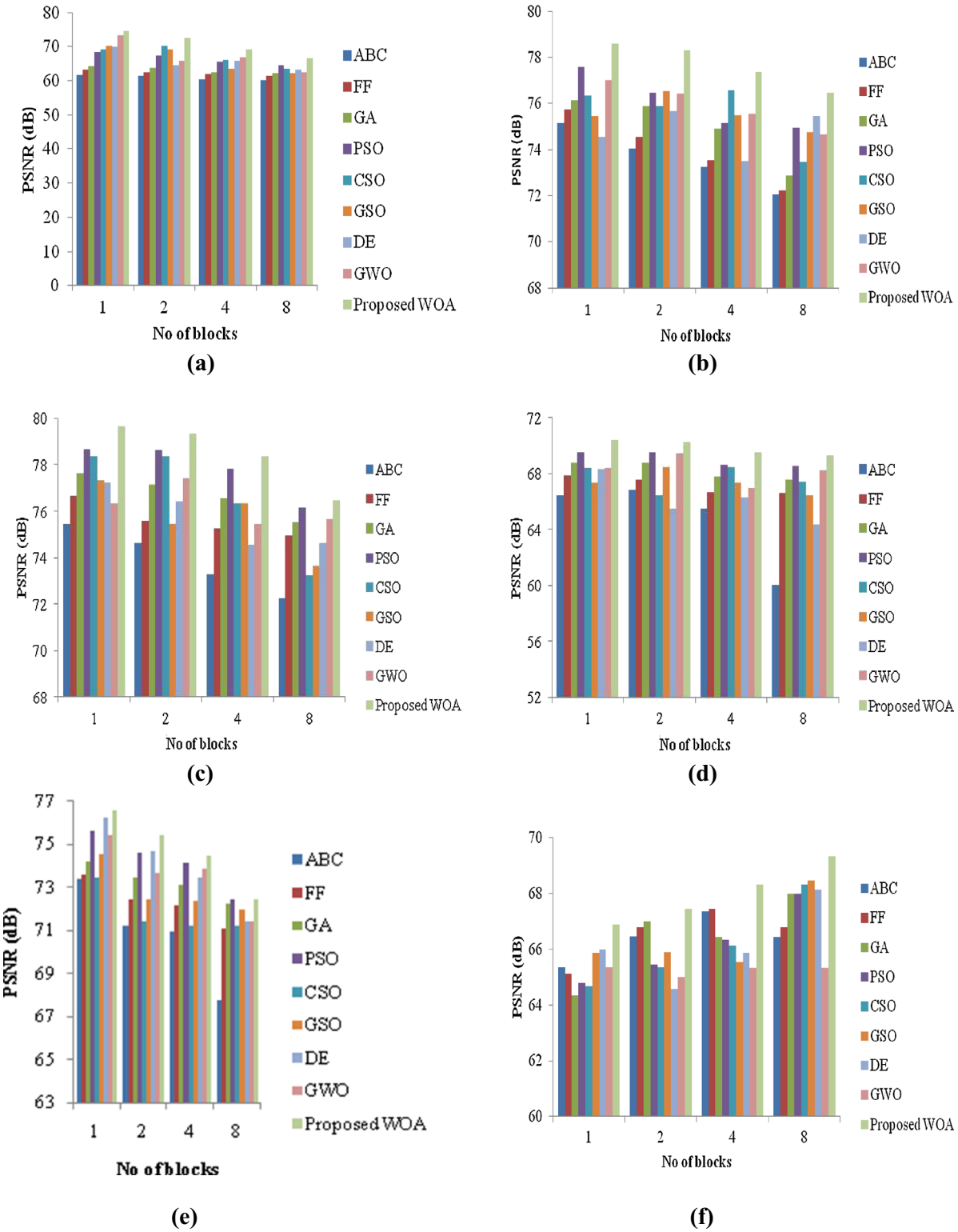

Fig. 5 Encoding performance of the proposed and conventional models with respect to PSNR for data set 1. **a** Football, **b** mobile, **c** garden, **d** coastguard, **e** foreman and **f** tennis

performance in terms of bit rate in compressed form in compressed for the data set 1. From Fig. 4a, for block size 1 the bit rate in compressed form for presented WOA is 1.89% ((87.84–89.54)/89.54) better than ABC, 1.31% bet-

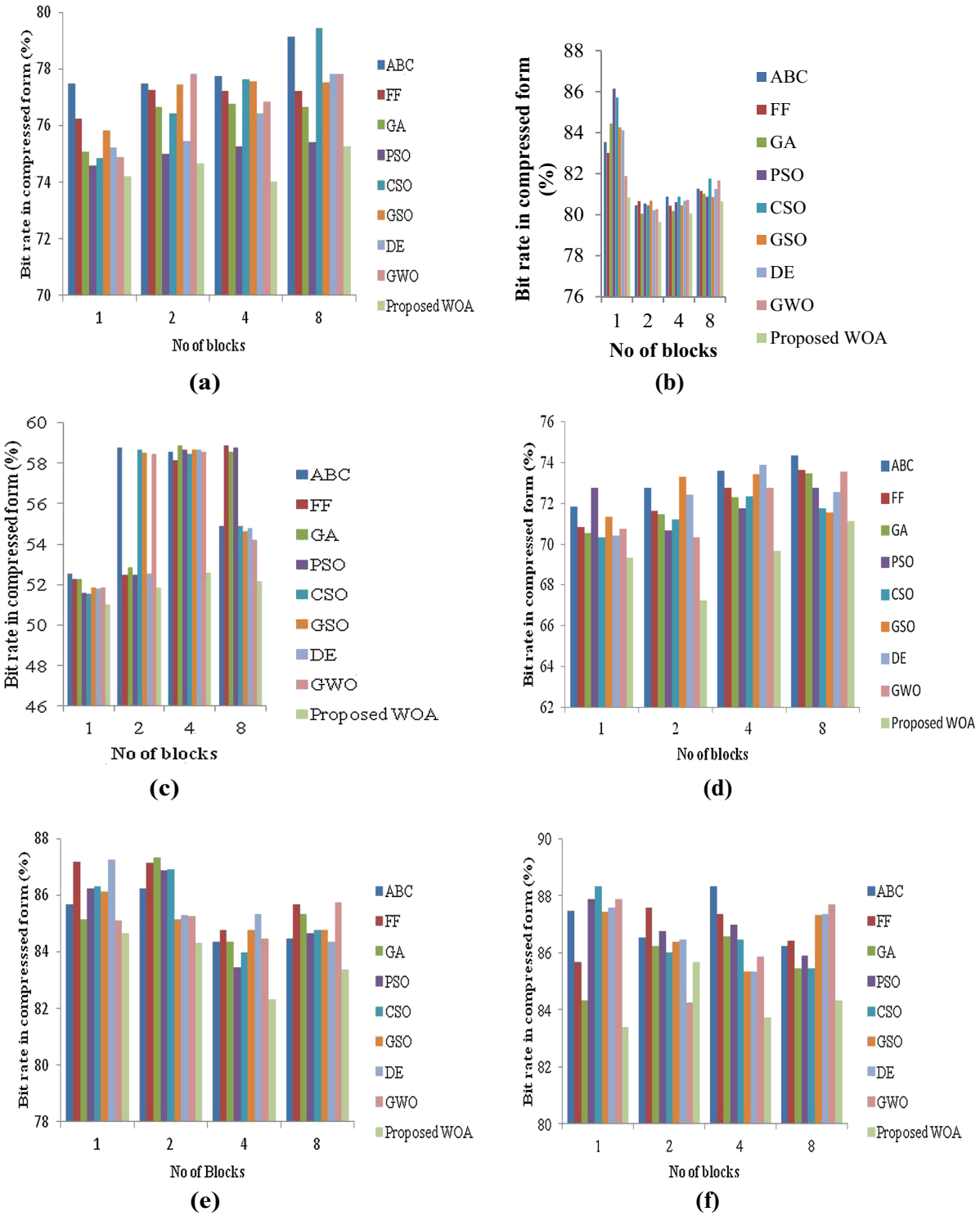

Fig. 6 Encoding performance of the proposed and conventional models with respect to Bit rate in compressed form for data set 2 **a** UHD HEVC-720p-30 Hz, **b** UHD HEVC-720p-60 Hz, **c** UHD HEVC-1080p-30 Hz, **d** UHD HEVC-1080p-60 Hz, **e** UHD HEVC-2160p-30 Hz and **f** UHD HEVC-2160p-60 Hz

ter than FF, 0.69% better than GA and 0.35% better than PSO algorithms. From Fig. 4b, for block size 2, the bit rate in compressed form for WOA is 3.57% better than ABC, 3.24% better than FF, 1.87% better than GA and 0.7% better than PSO algorithms. Also, from Fig. 4d, on considering block size 1, the presented WOA scheme is 0.68% better

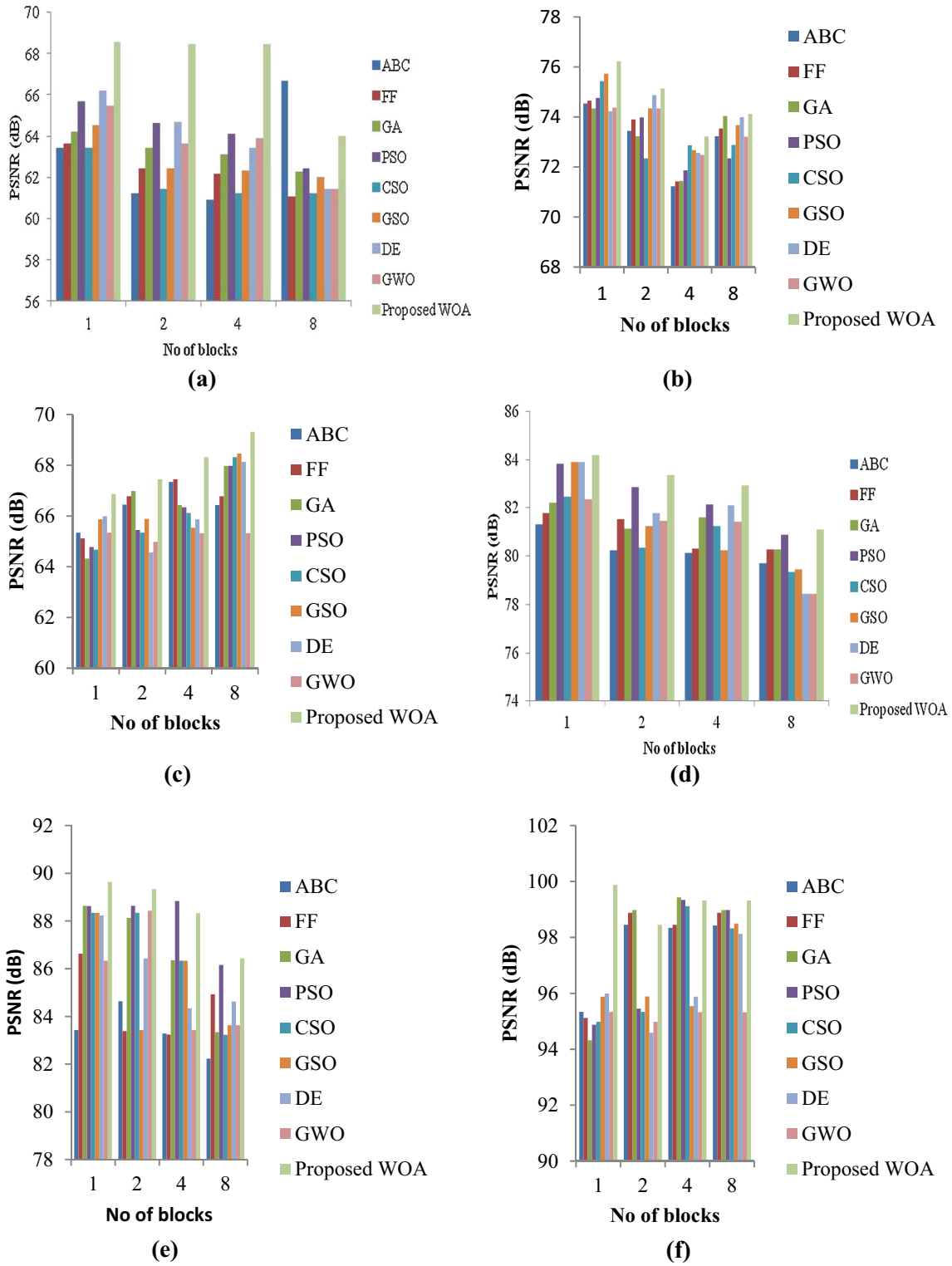

Fig. 7 Encoding performance of the proposed and conventional models with respect to PSNR for data set 2. **a** UHD HEVC-720p-30 Hz, **b** UHD HEVC-720p-60 Hz, **c** UHD HEVC-1080p-30 Hz, **d** UHD HEVC-1080p-60 Hz, **e** UHD HEVC-2160p-30 Hz and **f** UHD HEVC-2160p-60 Hz

than ABC, 0.23% better than FF, 0.98% better than GA and 0.81% better than PSO algorithms.

In Fig. 5a, the PSNR of the proposed method is 21.16% superior to ABC, 17.96% superior to FF, 15.81% superior to GA and 8.99% superior to PSO algorithms, 9.88% better than

Table 2 Performance analysis of the proposed and conventional methods for data set 1

Video sequences	SSIM								
	ABC	FF	GA	PSO	CSO	GSO	DE	GWO	Proposed method
Football	0.819	0.828	0.827	0.853	0.827	0.811	0.832	0.854	0.867
Garden	0.824	0.832	0.826	0.836	0.877	0.818	0.814	0.816	0.845
Mobile	0.837	0.843	0.835	0.821	0.822	0.825	0.842	0.841	0.856
Tennis	0.822	0.812	0.821	0.832	0.831	0.818	0.819	0.821	0.834
Coastguard	0.845	0.843	0.823	0.846	0.832	0.821	0.827	0.836	0.854
Foreman	0.841	0.837	0.826	0.832	0.812	0.841	0.823	0.834	0.845
RMSE									
Football	0.7312	0.7237	0.7325	0.7322	0.7432	0.7432	0.7433	0.7342	0.7015
Garden	0.7432	0.7321	0.7321	0.7321	0.7321	0.7325	0.7322	0.7234	0.7035
Mobile	0.7433	0.7432	0.7457	0.7433	0.7123	0.7213	0.7234	0.7234	0.7043
Tennis	0.7325	0.7342	0.7344	0.7432	0.7544	0.7553	0.7443	0.7123	0.7043
Coastguard	0.7433	0.7332	0.7334	0.7321	0.7234	0.7224	0.7139	0.7124	0.7032
Foreman	0.7433	0.7644	0.7212	0.7125	0.7124	0.7165	0.7135	0.7535	0.7054
UQI									
Football	0.4443	0.4543	0.4987	0.4454	0.4885	0.4875	0.4917	0.4900	0.4945
Garden	0.4743	0.4710	0.4491	0.4529	0.4729	0.4455	0.4735	0.4412	0.4813
Mobile	0.4324	0.4432	0.4325	0.4718	0.4845	0.4734	0.4832	0.4613	0.4932
Tennis	0.4125	0.4548	0.4255	0.4781	0.4623	0.4434	0.4471	0.4632	0.4812
Coastguard	0.4745	0.4655	0.4445	0.4432	0.4124	0.4543	0.4543	0.4745	0.4824
Foreman	0.4347	0.4743	0.4535	0.4789	0.4843	0.4322	0.4454	0.4785	0.4954
VIF									
Football	0.0026	0.0027	0.0028	0.0030	0.0028	0.0035	0.0035	0.0029	0.0037
Garden	0.0021	0.0028	0.0025	0.0030	0.0024	0.0035	0.0033	0.0027	0.0036
Mobile	0.0030	0.0030	0.0026	0.0026	0.0028	0.0033	0.0031	0.0024	0.0035
Tennis	0.0027	0.0028	0.0026	0.0026	0.0029	0.003312‘	0.0035	0.0025	0.0037
Coastguard	0.0029	0.0028	0.0027	0.0022	0.0027	0.0031	0.0034	0.0024	0.0037
Foreman	0.0030	0.0028	0.0028	0.0028	0.0023	0.0035	0.0035	0.0028	0.0036
Bit rate (Kbps)									
Football	18,061	17,461	24,108	21,766	‘17,243	17,234	18,232	22,324	24,342
Garden	16,234	18,231	23,221	22,873	18,341	18,452	19,341	22,234	23,657
Mobile	16,121	18,342	18,423	21,213	19,234	19,212	19,242	21,243	22,192
Tennis	17,863	18,873	19,232	22,422	20,421	20,211	19,442	21,942	23,434
Coastguard	17,334	17,222	21,141	22,235	16,232	20,214	18,313	20,331	23,424
Foreman	16,231	19,345	22,434	21,251	17,213	20,361	18,766	20,442	21,234

the GWO. Accordingly, the PSNR of the adopted scheme is 5.7% superior to ABC, 9.34% superior to FF, 3.16% superior to GA and 2.4% superior to PSO algorithms in Fig. 5b. In Fig. 5d, the PSNR of the adopted WOA scheme is 6.92% superior to ABC, 4.13% superior to FF, 2.34% superior to GA and 0.66% superior to PSO algorithms.

Similarly, the outcomes of the encoding process for data set 2 are presented in Figs. 6 and 7, respectively. Finally, it is known from the experimental outcomes that the proposed WOA has better PSNR and a bit rate in compressed form when compared with the conventional schemes.

Table 2 summarizes the performance analysis of the proposed and conventional methods in terms of SSIM, RMSE, UQI, VIF, bit rate (Kbps), and it is tested for data set 1. The overall analysis shows that the proposed method outperforms the conventional algorithms. The result analysis shows that the performance of the proposed method possess lower RMSE than that of the conventional models. The results obtained by the proposed method are far better when comparing with the conventional methods in terms of UQI. Moreover, the performance analysis of the proposed method and conventional methods in terms of bit rate. From the table,

Table 3 Performance analysis of the proposed and conventional methods for data set 2

Video sequences	SSIM								
	ABC	FF	GA	PSO	CSO	GSO	DE	GWO	Proposed method
UHD HEVC-720p-30 Hz	0.8122	0.8434	0.8365	0.8194	0.8554	0.8342	0.8133	0.8292	0.8761
UHD HEVC-720p-60 Hz	0.8323	0.839	0.8543	0.8653	0.8343	0.8123	0.8313	0.833	0.8782
UHD HEVC-1080p-30 Hz	0.8232	0.8333	.0.8314	0.8330	0.8445	0.8142	0.8341	0.8422	0.8533
UHD HEVC-1080p-60 Hz	0.834	0.8535	0.8763	0.8131	0.8231	0.8131	0.8231	0.8342	0.8784
UHD HEVC-2160p-30 Hz	0.8314	0.8441	0.8311	0.8131	0.8231	0.8133	0.8423	0.8322	0.8543
UHD HEVC-2160p-60 Hz	0.8423	0.8312	0.8424	0.8421	0.8423	0.8413	0.8313	0.8131	0.8655
RMSE									
UHD HEVC-720p-30 Hz	0.7322	0.7128	0.7322	0.7388	0.7348	0.7344	0.7135	0.7199	0.7070
UHD HEVC-720p-60 Hz	0.7178	0.7436	0.7250	0.7255	0.7187	0.7135	0.7235	0.7368	0.7070
UHD HEVC-1080p-30 Hz	0.7235	0.7424	0.7242	0.7313	0.7424	0.7242	0.7242	0.7244	0.7122
UHD HEVC-1080p-60 Hz	0.7131	0.7131	0.7222	0.7323	0.7424	0.7424	0.7242	0.7242	0.7032
UHD HEVC-2160p-30 Hz	0.7424	0.7313	0.7413	0.7212	0.7232	0.7242	0.7353	0.7242	0.7121
UHD HEVC-2160p-60 Hz	0.7424	0.7424	0.7424	0.7242	0.7424	0.7224	0.7342	0.7424	0.7154
UQI									
UHD HEVC-720p-30 Hz	0.4459	0.4786	0.4459	0.4543	0.4785	0.4694	0.4457	0.4531	0.4845
UHD HEVC-720p-60 Hz	0.4548	0.4342	0.4784	0.4759	0.4443	0.4543	0.4473	0.4543	0.4849
UHD HEVC-1080p-30 Hz	0.4354	0.4242	0.4234	0.4324	0.4242	0.4342	0.4346	0.4344	0.4423
UHD HEVC-1080p-60 Hz	0.4242	0.4324	0.4333	0.4311	0.4434	0.4333	0.4333	0.4232	0.4433
UHD HEVC-2160p-30 Hz	0.4223	0.4323	0.4242	0.4223	0.4341	0.4311	0.4424	0.4424	0.4531
UHD HEVC-2160p-60 Hz	0.4224	0.4322	0.4324	0.4342	0.4232	0.4131	0.4313	0.4231	0.4432
VIF									
UHD HEVC-720p-30 Hz	0.0023	0.0025	0.0028	0.0022	0.0023	0.0035	0.0035	0.0028	0.0037
UHD HEVC-720p-60 Hz	0.0028	0.0028	0.0024	0.0023	0.0022	0.0035	0.0035	0.0026	0.0037
UHD HEVC-1080p-30 Hz	0.0023	0.0023	0.0022	0.0021	0.0024	0.0033	0.0023	0.0023	0.0025
UHD HEVC-1080p-60 Hz	0.0022	0.0022	0.0032	0.0021	0.0022	0.0023	0.0023	0.0022	0.0033
UHD HEVC-2160p-30 Hz	0.0022	0.0024	0.0022	0.0022	0.0023	0.0022	0.0033	0.0032	0.0034
UHD HEVC-2160p-60 Hz	0.0021	0.0031	0.0031	0.0031	0.0033	0.0031	0.0031	0.0031	0.0032
Bit rate (Kbps)									
UHD HEVC-720p-30 Hz	17,231	19,463	19,214	19,123	17,977	19,311	19,321	19,131	20,313
UHD HEVC-720p-60 Hz	16,322	19,242	22,134	18,244	18,1233	19,634	19,234	19,242	22,243
UHD HEVC-1080p-30 Hz	17,242	18,224	18,242	18,353	19,4242	18,313	18,331	18,131	20,313
UHD HEVC-1080p-60 Hz	19,131	20,8131	19,242	19,244	19,535	19,244	19,424	19,464	21,313
UHD HEVC-2160p-30 Hz	18,232	18,1313	18,242	18,223	18,242	19,424	19,242	19,242	20,131
UHD HEVC-2160p-60 Hz	17,313	17,131	17,313	18,332	18,233	18,242	19,313	19,423	20,131

it is noticed that the bit rate values for the proposed method is higher than that of the conventional methods.

Table 3 shows the performance analysis of the proposed and conventional models in terms of data set 2. Here, the performance analysis is of the proposed method and conventional methods by evaluating the VQI. The overall analysis illustrates the performance of the proposed method is superior to the conventional models.

Tables 4 and 5 demonstrate the variation of the PSNR and SSIM versus the SNR of the proposed method for data set 1 and 2. For ease of observation, we have computed the PSNR and SSIM values for video sequences. From the tables, it can be see that the proposed method clearly outperforms all the conventional methods in terms of the PSNR and SSIM metrics.

5.3 Computational complexity

This section portrays the time which is consumed by the proposed and conventional schemes for the encoding process and it is shown in Tables 6 and 7. From Table 6, on considering the football video, the techniques have consumed

Table 4 Performance analysis of the proposed method in terms of PSNR, SSIM versus SNR (dB) for data set 1

Video sequence	PSNR				
	− 10	− 5	0	5	10
Football	14.78	12.3989	15.4342	7.4234	5.2255
Garden	11.903	10.2727	12.2342	8.3344	14.3223
Mobile	16.112	8.2342	10.2428	11.34425	11.534
Tennis	14.576	14.2432	9.34242	8.32423	12.424
Coastguard	9.8863	11.2313	8.4322	9.42323	15.4225
Foreman	8.9976	9.7787	15.034	10.4232	16.2432
SSIM					
Football	0.57	0.78	0.954	0.927	0.851
Garden	0.86	0.55	0.935	0.906	0.820
Mobile	0.59	0.823	0.934	0.8829	0.7723
Tennis	0.5	0.327	0.796	0.698	0.831
Coastguard	0.867	0.981	0.786	0.8775	0.698
Foreman	0.874	0.782	0.584	0.772	0.7447

Table 5 Performance analysis of the proposed method in terms of PSNR, SSIM versus SNR for data set 2

Video sequence	PSNR				
	− 10	− 5	0	5	10
UHD HEVC-720p-30 Hz	7.432	7.724	11.344	11.423	13.424
UHD HEVC-720p-60 Hz	7.909	8.456	9.023	6.424	10.424
UHD HEVC-1080p-30 Hz	7.234	7.342	8.224	7.242	9.242
UHD HEVC-1080p-60 Hz	7.431	8.243	7.355	7.354	9.424
UHD HEVC-2160p-30 Hz	7.992	8.423	8.424	8.353	9.288
UHD HEVC-2160p-60 Hz	10.242	10.242	10.243	11.131	11.244
SSIM					
UHD HEVC-720p-30 Hz	0.868	0.773	0.832	0.831	0.891
UHD HEVC-720p-60 Hz	0.869	0.964	0.649	0.843	0.887
UHD HEVC-1080p-30 Hz	0.843	0.842	0.742	0.724	0.850
UHD HEVC-1080p-60 Hz	0.677	0.942	0.744	0.744	0.965
UHD HEVC-2160p-30 Hz	0.764	0.755	0.744	0.742	0.842
UHD HEVC-2160p-60 Hz	0.535	0.564	0.766	0.677	0.766
UHD HEVC-720p-30 Hz	0.766	0.755	0.644	0.655	0.788
UHD HEVC-2160p-60 Hz	0.535	0.674	0.766	0.824	0.866

the time of 7352525 ms, 7535655 ms, 7565415 ms and 7854611 ms for block sizes 1, 2, 4 and 8, correspondingly for data set 1. Likewise, Table 7 describes the time utilized for the encoding process by the UHD HEVC-720p-30 Hz, UHD HEVC-720p-60 Hz, UHD HEVC-1080p-30 Hz, UHD HEVC-1080p-60 Hz, UHD HEVC-2160p-30 Hz and UHD HEVC-2160p-60 Hz. Here, the computational complexity of the proposed method will be lesser than the other conventional models in both datasets for various block size such as 1,2, 4 and 8.

The computational complexity of the proposed method is stated in Eq. (14), where N denotes number of iterations, M denotes the population size, H denotes the HEVC functions.

$$\text{Computational complexity} = O(N * M * H) \tag{14}$$

5.4 Optimization details of algorithm convergence

Table 8 summarizes the review on optimization details included in algorithm convergence. The overall analysis of the proposed method as well as the conventional algorithms with parameters and its values were described. Here, the parameters used for every basic algorithms of both conventional methods such as ABC, FF, GA, PSO, CSO, GSO, DE and GWO and the proposed method were determined as shown below.

Table 6 Time consumed (in ms) for the encoding process of data set 1

Block size	Algorithms	Football	Garden	Mobile	Tennis	Coastguard	Foreman
1	ABC	7652528	6645647	9554465	5886790	8648498	8762155
	FF	7552527	6745648	9654466	5986788	8748499	8862187
	GA	7752529	6845647	9754467	5786787	8848490	8962190
	PSO	7852530	6945648	9854468	5686789	8948492	8962187
	CSO	7452532	6745649	9954469	5786787	8648496	8762167
	GSO	7652531	6645650	9754465	5886790	8748495	8862156
	DE	7952528	6845651	9654468	5986788	8848499	8662178
	GWO	7552527	6945647	9854467	5686789	8948497	8862198
	Proposed method	7352525	6545646	9454464	5486786	8548488	8562145
2	ABC	7635676	6846649	9667888	5957880	8944465	8978187
	FF	7735680	6646650	9767890	5957878	8744478	8998190
	GA	7835687	6846646	9767880	5957879	8844488	8988178
	PSO	7935667	6646670	9867888	5957877	8744498	8998190
	CSO	7735678	6746649	9967890	5957887	8644490	8988198
	GSO	7835659	6946647	9767882	5957898	8744478	8978189
	DE	7935678	6646648	9667883	5957890	8844498	8968188
	GWO	7735698	6946680	9867897	5957889	8944489	8998196
	Proposed method	7535655	6546644	9567878	5857876	8544448	8958174
3	ABC	7865490	6878887	9878600	5895500	8978876	8725995
	FF	7965487	6978890	9778700	5995867	8988975	8925999
	GA	7765419	6978895	9878588	5895678	8998677	8825990
	PSO	7665456	6878887	9578609	5795987	8988876	8925991
	CSO	7765489	6978890	9778809	5895933	8998987	8825997
	GSO	7865478	6878899	9678666	5995676	8978678	8825999
	DE	7965467	6978888	9978777	5895785	8988888	8925990
	GWO	7865487	6878879	9878878	5795952	8998987	8825989
	Proposed method	7565415	6778875	9278578	5695412	8998542	8625987
4	ABC	7854700	6967700	9652922	6892876	8985900	8754941
	FF	7954888	6867757	9752865	6992588	8995995	8854666
	GA	7954987	6767899	9852978	6792678	8975975	8954784
	PSO	7954977	6667967	9952678	6892897	8985981	8854789
	CSO	7954887	6867854	9852876	6992567	8995904	8754678
	GSO	7954877	6967934	9752987	6892890	8985967	8854567
	DE	7954988	6867745	9652789	6792567	8995913	8954999
	GWO	7954899	6967821	9852907	6892875	8975944	8754299
	Proposed method	7854611	6567577	9552553	6692458	8965887	8654182

5.5 Outliers removal rate

The outlier removal rate is determined as the number of bits that are dropped out as redundant information by the proposed holoentropy based encoding method. This metric is inversely proportional to the number of bits transmitted after encoding process.

Figure 8 summarizes the Outliers removal rate of the proposed models for data set 2 using various block size. The overall analysis shows that the proposed method outperforms were analyzed for UHD HEVC-720p-30 Hz, UHD HEVC-720p-60 Hz, UHD HEVC-1080p-30 Hz, UHD HEVC-1080p-60 Hz, UHD HEVC-2160p-30 Hz and UHD HEVC-2160p-60 Hz using the block size 1,2 4 and 8. The result of the analysis shows that the performance of the proposed method is better for the UHD HEVC-1080p-30 Hz in dataset 2.

Figure 9 summarizes the outliers removal rate of the proposed models for data sets 1 using various block size. The overall analysis shows that the proposed method outperforms were analyzed for football, mobile, garden, coastguard, foreman and tennis using the block size 1, 2 4 and 8. The

Table 7 Time consumed (in ms) for the encoding process of data set 2

Block size	Algorithms	UHD HEVC-720p-30 Hz	UHD HEVC-720p-60 Hz	UHD HEVC-1080p-30 Hz	UHD HEVC-1080p-60 Hz	UHD HEVC-2160p-30 Hz	UHD HEVC-2160p-60 Hz
1	ABC	6768999	7813787	6933789	7913566	6992789	6823789
	FF	6868908	7913789	6833678	7813888	6992634	6923567
	GA	6968957	7713987	6933904	7713987	6992782	6923987
	PSO	6968907	7613654	6833987	7613678	6992456	6823855
	CSO	6768945	7513456	6933890	7713876	6992678	6823789
	GSO	6868952	7413567	6833667	7813906	6992906	6923678
	DE	6968948	7713789	6933678	7913678	6992567	6823567
	GWO	6768975	7813907	6833678	7513823	6992789	6923905
	Proposed method	6668831	7213133	6733442	7113433	6982423	6723423
2	ABC	6823767	7931678	6932987	7931890	6924900	6924890
	FF	6923890	7831890	6932789	7831933	6924876	6924888
	GA	6923577	7731907	6932456	7731766	6924789	6924832
	PSO	6823905	7631887	6932888	7831855	6924567	6924753
	CSO	6923778	7731567	6932780	7531766	6924788	6924789
	GSO	6823567	7531654	6932667	7431577	6924884	6924245
	DE	6923876	7831734	6932900	7631788	6924907	6924846
	GWO	6823909	7931887	6932789	7731377	6924678	6924903
	Proposed method	6723489	7231234	6832343	7231313	6824242	6824234
3	ABC	6934977	7935906	6954678	7621634	6972888	692734
	FF	6934876	7835845	6854987	7721678	6972566	692890
	GA	6934888	7935456	6954755	7821890	6972896	692976
	PSO	6934567	7735780	6854866	7921765	6972567	692666
	CSO	6934890	7635345	6954908	7721677	6972764	692987
	GSO	6934732	7835980	6954697	7821907	6972903	692456
	DE	6934978	7935765	6854834	7521237	6972890	692734
	GWO	6934888	7835567	6854567	7621678	6972777	692745
	Proposed method	6834243	7535224	6754313	7321213	6872344	682423
4	ABC	6431878	7923907	6923877	7813400	6988976	69623753
	FF	6531999	7723699	6823909	7713678	6988708	69923890
	GA	6631567	7823678	6923898	7913888	6998664	69723975
	PSO	6531788	7923888	6823678	7813999	6998953	69823678
	CSO	6731908	7823909	6923788	7713789	6988874	69923567
	GSO	6931789	7723786	6823988	7613900	6998666	69823722
	DE	6831899	7823856	6923666	7613885	6988876	69723987
	GWO	6831678	7923908	6823888	7513732	6998675	69623820
	Proposed method	6131331	7623424	6723423	7113344	6978242	69423423

result analysis shows that the performance of the proposed method is better for the coastguard and hence the garden video sequence obtains the lower value in dataset 2.

6 Conclusion

This paper has presented an encoding process in HEVC using enhanced holoentropy for proficient compression. The process of encoding in the HEVC system was attained by enhanced holoentropy that was determined based on weight-

Table 8 Review on optimization details included in algorithm convergence

Optimization algorithms	Parameters	Values
ABC	Control parameters such as colony size (CS), limit for scout (L) and dimension of the problem (D)	CS = 6 L = (CS*D)/2 = 6 D = 2
FF	Three control parameters: Randomization parameter α, the attractiveness β, and the absorption coefficient γ	$\alpha = 0.5$, $\gamma = 1.0$, $\beta_{\min} = 0.2$, and $\beta_0 = 1.0$
GA	Population size (P) Arithmetic crossover (α) Random number (μ_i)	$P = 4$ $\alpha = 0.5$ μ_i [0,1]
PSO	compressive function (σ) Behavioral parameters (φ_p, φ_g)	$\sigma \rightarrow (0, 1)$ $\varphi_p = 0, \varphi_g = 0$
CSO	Random number (r) Selecting probability (P_i)	r = [0,1], $P_i = 1$
GSO	Gravitational constant (G) Active and passive gravitational masses (M_{ai} and M_{pi})	$G = 6.674\,30 \times 10^{-11}$ m^3 kg^{-1} s^{-2}
DE	Random value, Initial (rand), population (P_0), Population size (N_p)	rand(0,1), P_0:1, $N_p = 30$
GWO	Random numbers (r_1, r_2), position of the prey (t) Fitness function (α, β, δ)	r_1, r_2 = [0, 1] $t = 0$
Proposed method	Random vector ($\vec{r}$), Random value of prey (P_a)	$\vec{r}$ = [0, 1] P_a = [0,1]

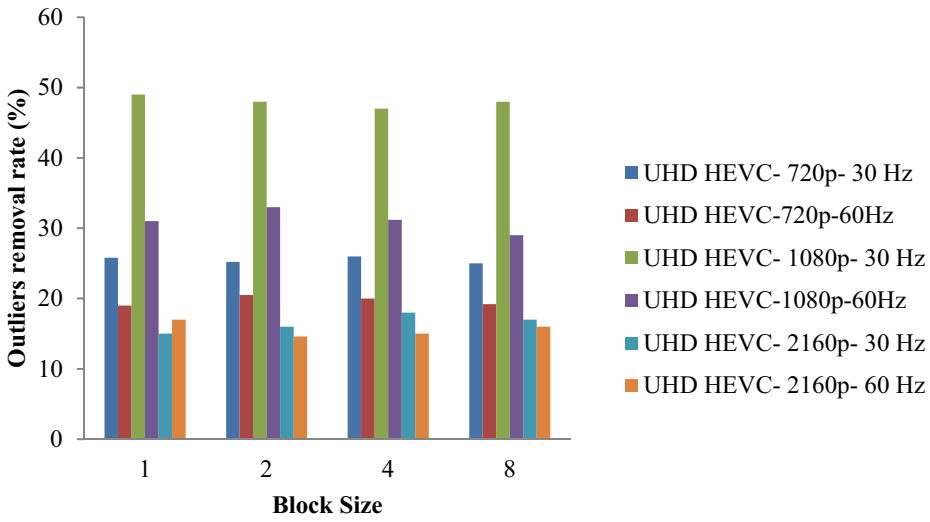

Fig. 8 Outliers removal rate (%) of the proposed models for data set 2 using various block size

ing tansig function. Accordingly, the weights of tansig function were optimally tuned using the WOA algorithm. When high-resolution video sequences were processed, it needs considerable development. The pixel deviations beneath altering frames were clustered depending on the interest, and accordingly, the outliers were eliminated using a sophisticated entropy standard known as enhanced holoentropy. Moreover, the adopted approach was distinguished with the traditional techniques namely, ABC, FF, PSO GA, CSO, GSO, DE and GWO in terms of PSNR, bit rate in compressed form, RMSE, SSIM, UQI, VIF and bit rate. From the analysis, for block size 1, the bit rate in compressed form for presented WOA was 1.89% better than ABC, 1.31% better than FF, 0.69% better than GA and 0.35% better than PSO algorithms. Likewise, the PSNR for offered WOA was 21.16% superior to ABC, 17.96% superior to FF, 15.81% superior to GA and 8.99% superior to PSO algorithms. Likewise, considering the football video in terms of time consumption analysis, the techniques have consumed the time of 7352525 ms, 7535655 ms, 7565415 ms and 7854611 ms for

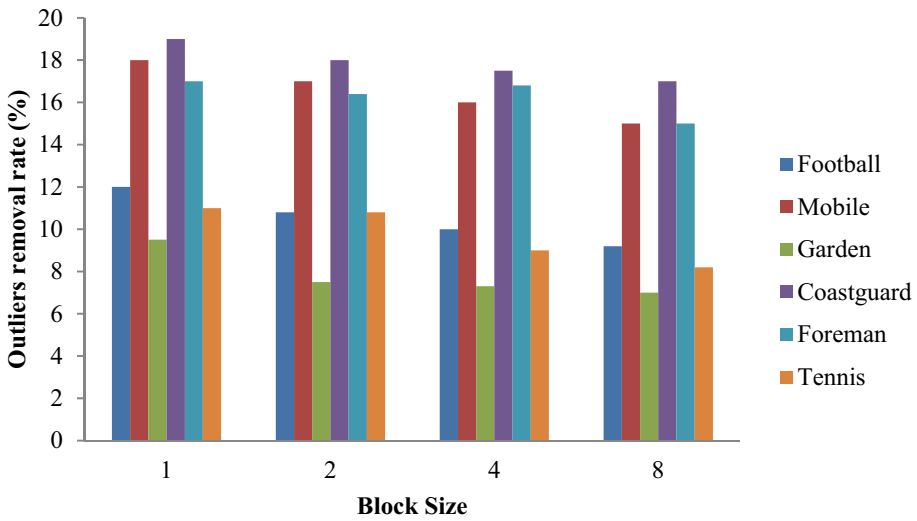

Fig. 9 Outliers removal rate (%) of the proposed models for data set 1 using various block size

block sizes 1, 2, 4 and 8, correspondingly. Thus, by performing the encoding procedure, the proposed model was found to minimize the size of a video with perceptually enhanced PSNR or video quality with reduced computational time.

Compliance with ethical standards

Conflict of interest The authors declare that they have no conflict of interest.

Ethical approval This paper does not contain any studies with human participants or animals performed by any of the authors.

References

1. Lin, J.L., Chen, Y.W., Chang, Y.L., An, J., Lei, S.: Advanced texture and depth coding in 3D-HEVC. J. Vis. Commun. Image Represent. **50**, 83–92 (2018)
2. Pan, Z., Jin, P., Lei, J., Zhang, Y., Sun, X., Kwong, S.: Fast reference frame selection based on content similarity for low complexity HEVC encoder. J. Vis. Commun. Image Represent. **40**, 516–524 (2016)
3. Migallón, H., Hernández-Losada, J.L., Cebrián-Márquez, G., Piñol, P., Malumbres, M.P.: Synchronous and asynchronous HEVC parallel encoder versions based on a GOP approach. Adv. Eng. Softw. **101**, 37–49 (2016)
4. Mercat, A., Bonnot, J., Pelcat, M., Desnos, K., Menard, D.: Smart search space reduction for approximate computing: a low energy HEVC encoder case study. J. Syst. Arch. **80**, 56–67 (2017)
5. Lee, D., Jeong, J.: Fast CU size decision algorithm using machine learning for HEVC intra coding. Signal Process. Image Commun. **62**, 33–41 (2018)
6. Shen, L., Zhang, Z., Zhang, X., An, P., Liu, Z.: Fast TU size decision algorithm for HEVC encoders using Bayesian theorem detection. Signal Process. Image Commun. **32**, 121–128 (2015)
7. Zhang, Q., Wang, X., Huang, X., Rijian, S., Gan, Y.: Fast mode decision algorithm for 3D-HEVC encoding optimization based on depth information. Digit. Signal Process. **44**, 37–46 (2015)
8. Guarda, A.F., Santos, J.M., da Silva Cruz, L.A., Assunção, P.A., Rodrigues, N.M., de Faria, S.M.: A method to improve HEVC lossless coding of volumetric medical images. Signal Process. Image Commun. **59**, 96–104 (2017)
9. Fernández, D.G., Del Barrio, A.A., Botella, G., García, C., Hermida, R.: Complexity reduction in the HEVC/H265 standard based on smooth region. Digit. Signal Process. **73**, 24–39 (2018)
10. Sole, J., Joshi, R., Nguyen, N., Ji, T., Karczewicz, M., Clare, G., Duenas, A.: Transform coefficient coding in HEVC. IEEE Trans. Circuits Syst. Video Technol. **22**(12), 1765–1777 (2012)
11. Kıran, M.S., Fındık, O.: A directed artificial bee colony algorithm. Appl. Soft Comput. **26**, 454–462 (2015)
12. González-de-Suso, J.L., Martínez-Enríquez, E., Díaz-de-María, F.: Adaptive Lagrange multiplier estimation algorithm in HEVC. Signal Process. Image Commun. **56**, 40–51 (2017)
13. Llamocca, D.: Self-reconfigurable architectures for HEVC forward and inverse transform. J. Parallel Distrib. Comput. **109**, 178–192 (2017)
14. Mirjalili, S., Lewis, A.: The whale optimization algorithm. Adv. Eng. Softw. **95**, 51–67 (2016)
15. Sullivan, G., Ohm, J., Han, W.-J., Wiegand, T.: Overview of the high efficiency video coding (HEVC) standard. IEEE Trans. Circuits Syst. Video Technol. **22**(12), 1649–1668 (2012)
16. Sullivan, G.J., Boyce, J.M., Chen, Y., Ohm, J.R., Segall, C.A., Vetro, A.: Standardized extensions of high efficiency video coding (HEVC). IEEE J. Select. Top. Signal Process. **7**(6), 1001–1016 (2013)
17. Mostafa Bozorgi, S., Yazdani, S.: IWOA: an improved whale optimization algorithm for optimization problems. J. Comput. Des. Eng. **6**(3), 243–259 (2019)
18. Liu, Z., Lin, T.-L., Chou, C.-C.: Efficient prediction of CU depth and PU mode for fast HEVC encoding using statistical analysis. J. Vis. Commun. Image Represent. **38**, 474–486 (2016)
19. Xu, Z., Min, B., Cheung, R.C.: A fast inter CU decision algorithm for HEVC. Signal Process. Image Commun. **60**, 211–223 (2018)
20. Masera, M., Fiorentin, L.R., Masala, E., Masera, G., Martina, M.: Analysis of HEVC transform throughput requirements for hardware implementations. Signal Process. Image Commun. **57**, 173–182 (2017)
21. Tang, T., Li, L.: Rate control for non-uniform video in HEVC. J. Vis. Commun. Image Represent. **48**, 254–267 (2017)
22. Chung, B., Yim, C.: Fast intra prediction method by adaptive number of candidate modes for RDO in HEVC. Inf. Process. Lett. **131**, 20–25 (2018)

23. Ding, H., Huang, X., Zhang, Q.: The fast intra CU size decision algorithm using gray value range in HEVC. Opt. Int. J. Light Electron Opt. **127**(18), 7155–7161 (2016)
24. Kuanar, S., Rao, K.R.: Christopher conly, fast mode decision in HEVC intra prediction, using region wise CNN feature classification. In: International Conference on Multimedia and Expo Workshops (ICMEW), San Diego, CA, pp. 1–4. IEEE (2018)
25. Kuanar, S., Rao, K.R., Bilas, M., Bredow, J.: Adaptive CU mode selection in HEVC intra prediction: a deep learning approach. Circuits Syst. Signal Process. **38**(11), 5081–5102 (2019)
26. Kuanar, S., Conly, C., Rao, K.R.: Deep learning based HEVC in-loop filtering for decoder quality enhancement. In: Picture Coding Symposium (PCS), pp 164-168. IEEE (2018)
27. Goswami, K., Lee, J.H., Kim, B.G.: Fast algorithm for the high efficiency video coding (HEVC) encoder using texture analysis. Inf. Sci. **364**, 72–90 (2016)
28. Dutta, T., Gupta, H.P.: A robust watermarking framework for high efficiency video coding (HEVC)-encoded video with blind extraction process. J. Vis. Commun. Image Represent. **38**, 29–44 (2016)
29. Zhang, Q., Zhang, Z., Jiang, B., Zhao, X., Gan, Y.: Fast 3D-HEVC encoder algorithm for multiview video plus depth coding. Opt. Int. J. Light Electron Opt. **127**(20), 8864–8873 (2016)
30. Lin, T.-L., Yang, N.-C., Syu, R.-H., Liao, C.-C., Chen, S.-L.: NR-bitstream video quality metrics for SSIM using encoding decisions in AVC and HEVC coded videos. J. Vis. Commun. Image Represent. **32**, 257–271 (2015)
31. Guo, J., Gong, H., Weijian, X., Huang, L.: Hierarchical content importance-based video quality assessment for HEVC encoded videos transmitted over LTE networks. J. Vis. Commun. Image Represent. **43**, 50–60 (2017)
32. Wang, S., Luo, F., Ma, S., Zhang, X., Gao, W.: Low complexity encoder optimization for HEVC. J. Vis. Commun. Image Represent. **35**, 120–131 (2016)
33. Van, X.H., Ascenso, J., Pereira, F.: HEVC backward compatible scalability: a low encoding complexity distributed video coding based approach. Signal Process. Image Commun. **33**, 51–70 (2015)
34. Kumar, B.S., Manjunath, A.S., Christopher, S.: Improved entropy encoding for high efficient video coding standard. Alex. Eng. J. **57**(1), 1–9 (2018)
35. Choi, Y.J., Jun, D.S., Cheong, W.S., Kim, B.G.: Design of efficient perspective affine motion estimation/compensation for versatile video coding (VVC) standard. Electronics **8**(9), 993 (2019). https://doi.org/10.3390/electronics8090993
36. Yang, R., Xu, M., Wang, Z.: Decoder-side HEVC quality enhancement with scalable convolutional neural network. In: IEEE International Conference on Multimedia and Expo (ICME), Hong Kong, pp. 817–822 (2017). https://doi.org/10.1109/icme.2017.8019299
37. Lee, J.H., Lee, Y.W., Jun, D., Kim, B.G.: Efficient color artifact removal algorithm based on high-efficiency video coding (HEVC) for high-dynamic range video sequences. IEEE Access **8**, 64099–64111 (2020). https://doi.org/10.1109/access.2020.2984012
38. Goswami, K., Kim, B.G.: A design of fast high-efficiency video coding scheme based on markov chain monte carlo model and Bayesian classifier. IEEE Trans. Ind. Electron. **65**(11), 8861–8871 (2018). https://doi.org/10.1109/tie.2018.2815941
39. Jin, Z., An, P., Yang, C., Shen, L.: Quality enhancement for intra frame coding via CNNS: an adversarial approach. In: ICASSP, pp. 1368–1372 (2018)
40. Lee, Y.W., Kim, J.H., Choi, Y.J., Kim, B.G.: CNN-based approach for visual quality improvement on HEVC. In: IEEE International Conference on Consumer Electronics (ICCE 2018), pp. 498–500 (2018)
41. Fister, I., Fister, I., Yang, X.-S., Brest, J.: A comprehensive review of firefly algorithms. Swarm Evolut. Comput. **13**, 34–46 (2013)
42. McCall, J.: Genetic algorithms for modelling and optimisation. J. Comput. Appl. Math. **184**(1), 205–222 (2005)
43. Zhang, J., Xia, P.: An improved PSO algorithm for parameter identification of nonlinear dynamic hysteretic models. J. Sound Vib. **389**, 153–167 (2017)
44. Sarangi, A., Sarangi, S.K., Mukherjee, M., Panigrahi, S.P.: System identification by Crazy-cat swarm optimization. In: 2015 International Conference on Microwave, Optical and Communication Engineering (ICMOCE), pp. 439–442. IEEE (2015)
45. Hatamlou, A., Abdullah, S., Othman, Z.: Gravitational search algorithm with heuristic search for clustering problems. In: 2011 3rd Conference on Data Mining and Optimization (DMO), Putrajaya, pp. 190–193 (2011)
46. Mohamad, Z.S., Darvish, A., Rahnamayan, S.: Eye illusion enhancement using interactive differential evolution. In 2011 IEEE Symposium on Differential Evolution (SDE), pp. 1–7. IEEE (2011)
47. Gu, W., Zhou, B.: Improved grey wolf optimization based on the quantum-behaved mechanism. In: 2019 IEEE 4th Advanced Information Technology, Electronic and Automation Control Conference (IAEAC), Chengdu, China, pp. 1537–1540 (2019)

Venkatesh Munagala received B.Tech. (ECE) degree from JNTU, Hyderabad, Andhra Pradesh, India, in 2008 and M.Tech. (VLSI Design) from NITK, Surathkal, Karnatak, India, in 2011. He is presently pursuing part-time Ph.D. at JNTU Kakinada and has more than 9 years of experience in teaching. His current research includes digital image and video processing and VLSI design. At present, he is an Assistant Professor in the Department of ECE, VVIT, Nambur, Andhra Pradesh.

Satya Prasad Kodati received B.Tech. (ECE) degree from JNT university, Hyderabad, Andhra Pradesh, India, in 1977, M.E. (Communication systems) from University of Madras, India, in 1979 and Ph.D. from IIT Madras, India, in 1989. He has more than 35 years of experience in teaching and 20 years in R&D. His current research interests include signals and systems, communications, digital signal processing, RADAR and telemetry. He received patent for his research work in 2015.